Available online at www.sciencedirect.com
ScienceDirect
Journal of Power Sources 167 (2007) 1–10
JOURNAL OF POWER SOURCES
www.elsevier.com/locate/jpowsour

Electroactivity of tin modified platinum electrodes for ethanol electrooxidation

F.C. Simões [b], D.M. dos Anjos [a], F. Vigier [a], J.-M. Léger [a], F. Hahn [a], C. Coutanceau [a], E.R. Gonzalez [c], G. Tremiliosi-Filho [c], A.R. de Andrade [b], P. Olivi [b], K.B. Kokoh [a,*]

[a] *Equipe Electrocatalyse, UMR 6503 CNRS, Université de Poitiers, 40 Avenue du Recteur Pineau, 86022 Poitiers Cedex, France*
[b] *Departamento de Quimica da Faculdade de Filosofia, Ciências e Letras de Ribeirão Preto, Universidade de São Paulo, Av. Bandeirantes, Caixa Postal 3900, 14040-901 Ribeirão Preto, SP, Brazil*
[c] *Instituto de Quimica de São Carlos, Universidade de São Paulo, Caixa Postal 780, 13560-970 São Carlos, SP, Brazil*

Received 10 July 2006; received in revised form 21 September 2006; accepted 7 December 2006
Available online 11 February 2007

Abstract

Different electrochemical techniques like cyclic voltammetry and chronoamperometry and tests in a single direct ethanol fuel cell (DEFC) were used to evaluate the catalytic activity of various compositions of PtSn electrodes prepared by thermal decomposition for ethanol electrooxidation. This oxidation process was also investigated by in situ infrared reflectance spectroscopy to determine the presence of adsorbed intermediates. The experimental results showed that PtSn can oxidize ethanol mainly to acetaldehyde and acetic acid. Adsorbed CO was also found, which demonstrates that the rupture of the C–C bond in the ethanol molecule can also take place during the oxidation process. This intermediate species was oxidized to CO_2 which was detected by IR spectroscopy and chromatography. With $Pt_{90}Sn_{10}$/C as anode catalyst, single DEFC tests carried out using MEAs with a geometric electrode area of 5 cm^2 allowed to produce a power density of ca. 72 mW cm^{-2} at 110 °C.

Keywords: Ethanol oxidation; DEFC; Platinum-tin electrocatalyst

1. Introduction

The proton exchange membrane fuel cell (PEMFC) is one of the most promising electrochemical devices for energy generation that can be applied in electrical vehicles and portable electronic devices. Up to now the best performance has been reached using hydrogen as a fuel. This fuel can be supplied either directly from a storage tank or indirectly from liquid substances through a reformer. However, the problems found in the storage, handling, and distribution of hydrogen are important barriers to its direct use. The costs and the extra weight of the equipment used in hydrogen FCs are also important problems when reformers are used. For all these reasons, the direct use of liquid fuels in the cell has been investigated as a convenient alternative to hydrogen. The most important substances considered in this case have been low molecular weight alcohols, mainly methanol and ethanol [1–7]. The use of the latter is attractive since it is less toxic when compared with methanol, and it is also produced from renewable sources. However, the rupture of the C–C bond is not easy to promote by electrochemical means, posing difficulties to the development of direct ethanol fuel cells (DEFC). Partial oxidation of ethanol can lead to the formation of acetaldehyde and acetic acid, which means a decrease in the electrical cell efficiency [8–10]. Therefore, the development of a catalyst that oxidizes ethanol efficiently at low potentials is of high interest. Pt alloys are promising electrode materials for this purpose. Among the metals investigated to form alloys with Pt, tin led to interesting results, although some contradictory results can be found in the literature. Jiang et al. demonstrated that the tin oxidation state plays an important role in determining the influence of tin on the Pt activity and on electrode stability [11]. According to the authors, higher oxidation states may favor ethanol electrooxidation. Sn or its oxides can supply surface oxygen-containing species for the oxidative removal of CO-like species strongly adsorbed on adjacent Pt active sites, the so-called bifunctional mechanism, and activate

* Corresponding author. Tel.: +33 549 45 41 20; fax: +33 549 45 35 80.
E-mail address: boniface.kokoh@univ-poitiers.fr (K.B. Kokoh).

0378-7753/$ – see front matter © 2007 Elsevier B.V. All rights reserved.
doi:10.1016/j.jpowsour.2006.12.113

the chemisorbed CO-like intermediates. The tin oxidation state may depend on the preparation method and the investigation and evaluation of different methods may help to understand the electrode process and point the direction for the development of highly active materials.

The literature shows clearly a continuous effort toward the development of different synthetic methods based on colloids [6,12], microemulsions [13,14], sonochemistry [15], and microwave irradiation [16], with the purpose of improving the catalytic activity of electrode materials. In this work, it is proposed the use of an alternative method, called the Pechini method [17], for the preparation of Pt-Sn electrodes. This method is based on the thermal decomposition of polymeric precursors obtained by the polymerization reaction between a hydrocarboxylic acid and a polyhydroxylic alcohol. In this method, appropriate salts of the desired metals are dissolved in the precursor solution, and it is possible to obtain catalytic materials in the form of thin films or as powders of high surface area. In this work, catalysts containing Pt and Sn were prepared and characterized by XRD, TEM and EDX. Their catalytic activity toward ethanol electrooxidation was studied by chronoamperometry. DEFC tests were made with membrane electrode assemblies (MEAs) prepared by hot pressing a pretreated Nafion® 117 membrane together with a Pt-Sn anode and an E-TEK cathode.

2. Experimental

2.1. Synthesis and characterization of the catalysts

Pt-based electrocatalysts with various amounts of Sn were prepared from appropriate molar ratios at 10% intervals by thermal decomposition of polymeric precursors [17–19]. Both thin films deposited on a Ti substrate and powder samples of nominal composition $Pt_xSn_{(1-x)}O_2$, where $0.50 < x < 0.9$, were used in this work. The tin polymeric precursor (Sn-resin) was prepared by mixing citric acid (CA) (Merck) in ethylene glycol (EG) (Merck) at 60–65 °C. After total dissolution of CA the temperature was raised to 90 °C and a tin citrate (TC) solution (0.1 mol dm^{-3} in isopropanol prepared as described elsewhere [20]) was then added. The molar ratios CA:EG:TC were 3:10:1. The platinum polymeric precursor (Pt-resin) was prepared in a similar way, but the molar ratio AC:EG:H_2PtCl_6 was 4:16:1. Precursor mixtures were prepared for each electrode composition by dissolving the appropriate amounts of Sn-resin (3.5×10^{-3} mol Sn g^{-1} resin) and Pt-resin (3.8×10^{-4} mol Pt g^{-1} resin). The precursor mixtures were applied by brushing on both sides of the Ti-support, previously sandblasted and chemically treated in hot aqueous oxalic acid 10% (w/w) for 30 min and then washed with Milli-Q water and dried at 130 °C. After the application of each coating, the electrode was heated in air at 130–140 °C for 10 min to polymerize the coating, and then calcinated at 400 °C for 5 min. This procedure was repeated until the desired nominal oxide loading (1.4–1.6 mg cm^{-2}) was reached. The layers were finally annealed for 1 h, at 400 °C, under O_2-flux. Duplicate samples were prepared for each electrode composition. Thin films deposited on a 2 cm^2 Ti substrate were used for the voltammetric and chronoamperometric experiments.

Complete fuel cell measurements were carried out on electrocatalysts dispersed on carbon Vulcan XC-72. Powder samples were also prepared by thermal decomposition of the polymeric precursor mixtures. The mixture of carbon and metallic resin was dispersed in 2 mL of water in an ultrasonic bath, dried and then calcinated using the following temperature program: the temperature was raised initially at 2 °C min^{-1} until 250 °C hold at this temperature for 1 h and after that ramped at 10 °C min^{-1} until 350 °C min^{-1} (30 min) and finaly 30 °C min^{-1} until the final temperature (400 °C) was achieved. The sample was kept at the final temperature for 2 h.

The catalysts were characterized by X-ray diffraction (XRD) using a Bruker D8 Advance diffractometer operating with Cu Kα radiation ($\lambda = 0.15406$ nm) generated at 40 kV and 40 mA. Steps of 0.0246° with time/step of 0.1 s for 2θ values between 20 and 70° were employed.

The morphology of the different Pt-Sn/C electrodes materials was examined by transmission electron microscopy (TEM) using a Philips CM 120 microscope. Energy dispersive X-rays analysis (EDX) was used to estimate the composition of the nanoparticles.

The electrochemical activity of the materials was examined by cyclic voltammetry in a thermostated three-electrode cell. The electrochemical measurements were performed on a PC controlled VoltaLab Potentiostat PGZ 420 Electrochemical Interface. A reversible hydrogen electrode (RHE) and a slab of vitreous carbon were used as reference and counter electrode, respectively. The electrochemical surface area of the electrodes was obtained from the integration of the hydrogen adsorption/desorption region.

2.2. Electrolysis of ethanol and chromatographic analysis of the reaction products

A three-electrode Pyrex cell, with two identical compartments (15 cm^3 each compartment) separated by an ion-exchange membrane (Nafion® 423), was used to perform the chronoamperometric experiments. A Pt-Ir grid served as the counter electrode. The electrolysis reaction product yield was followed by high performance liquid chromatography (HPLC), using a double online detection system with UV ($\lambda = 210$ nm) and refractive index detectors. An Aminex HPX-87H column from Bio-Rad was used and the eluent was a 1 mM H_2SO_4 solution at a 0.6 cm^3 min^{-1} flow rate. Identification of the products was performed comparing retention times with those of commercially available standards. The products formed during the bulk electrooxidation of ethanol were determined by comparing their retention times with those of pure reference products under the same conditions. During chronoamperometric experiments, the carbon dioxide formed was trapped in a cell containing 0.1 M NaOH (1 mL). At the end of the experiment, nitrogen was bubbled in the cell to remove all the CO_2 towards the trap cell. Carbonate was analyzed quantitatively by comparison with a Na_2CO_3 reference prepared under the same condition.

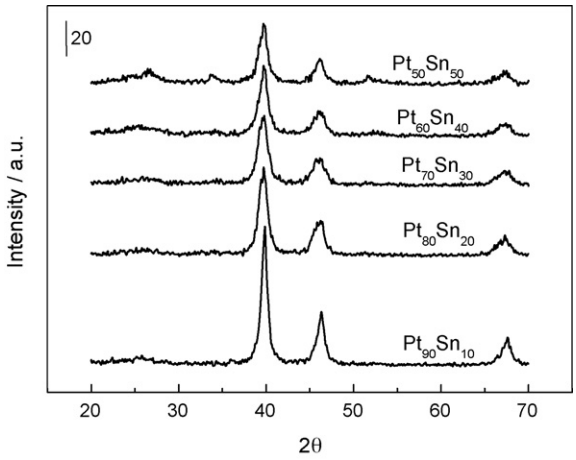

Fig. 1. XRD diffractogram of Pt-Sn/C electrocatalysts (30% metal loading) prepared by thermal decomposition of polymeric precursors.

2.3. Preparation of the electrodes and the membrane/electrode assemblies

The membrane electrode assemblies (MEAs) were prepared by hot pressing a pretreated Nafion® 117 membrane placed between an E-TEK Pt cathode (2 mg cm^{-2} metal loading, 40 wt.%) and a home-made anode (2 mg cm^{-2} metal loading 30 wt.%) at 130 °C for 90 s under a pressure of 35 kg cm^{-2}. The procedure for the electrode fabrication was described elsewhere [6]. The operating fuel cell performance was determined in a single DEFC with a 5 cm^2 geometric surface area of electrodes using a Globe Tech test bench. The $E=f(j)$ and $P=f(j)$ curves were recorded on a high power potentiostat (Wenking model HP 88) interfaced with a PC.

2.4. IR spectroscopic measurements

IR spectroscopy measurements were performed on catalysts supported on a gold substrate in order to obtain a better reflectivity. The precursor solutions were applied onto the substrate by painting followed by heating at 150 °C for 5 min, and then at 400 °C for 5 min. This procedure was repeated until a desired mass corresponding to a nominal thickness of 2 μm was obtained. When this condition was achieved, the electrodes were calcinated in air at 450 °C for 1 h to eliminate the organic materials used to produce the metallic film.

The Fourier transform IR spectrometer used here was a Bruker IFS 66v, with the sample compartment modified to allow the beam to be reflected on the electrode surface with an incidence angle of 65°, after passing through the IR window (CaF_2) of a conventional thin layer spectroelectrochemical cell. The beam path was under vacuum and a liquid N_2 cooled HgCdTe detector (Infrared Associates) was used.

3. Results and discussion

3.1. Physico-chemical characterization of the catalysts

Various powder samples of the Pt-Sn catalysts supported on Vulcan XC-72 carbon black were studied by XRD, TEM and EDX analyses. XRD patterns for the as-prepared Pt-Sn catalysts are depicted in Fig. 1. As can be seen, the pattern shows the characteristic peaks of both, the face-centered cubic (fcc) crystalline Pt and of the SnO_2. Small peaks for SnO_2 were clearly found at 26.8, 33.9 and 51.9° for Pt-Sn (50:50). In spite of these peaks are not clearly observed in the corresponding diffractograms for the other catalysts, the presence of tin oxides cannot be discarded because it may be present in a small amount or even in an amorphous form. The presence of metallic platinum is clearly revealed by the characteristic diffraction peaks of Pt [1 1 1], [2 0 0] and [2 2 0] planes at 2Θ values of 39.7, 46.2 and 67.4°, respectively. On the basis of comparison they are in agreement with the peaks for pure Pt and SnO_2. We did not find clear evidences for the formation of a PtSn solid solution since no noticeable shifts in the Pt peaks positions were noted neither other peaks. Metallic Sn was not formed in the catalyst prepared by thermal decomposition of polymeric precursors. A possible mixture of two phases, SnO_2 and Pt, dominates the catalyst. The presence of solid solutions were not found but more detailed studies should be addressed to clarify this point.

TEM showed that the obtained nanoparticles are well dispersed on the Vulcan support (Figs. 2 and 3). It can be seen that

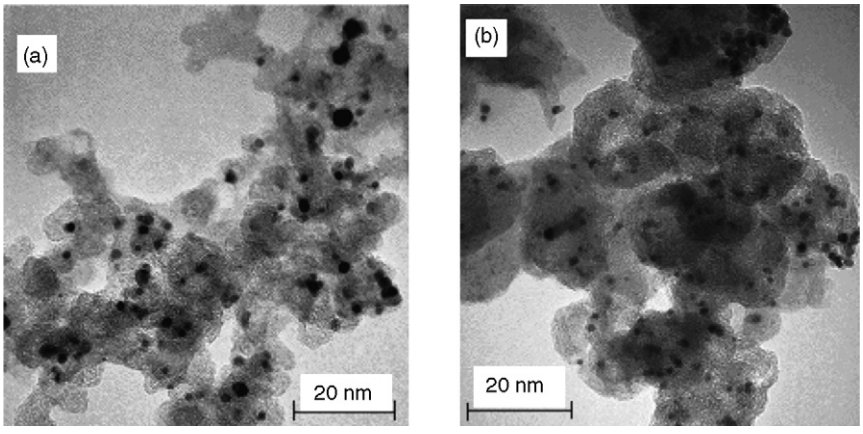

Fig. 2. TEM images of Pt-Sn/C electrocatalysts (30% metal loading) prepared by thermal decomposition of polymeric precursors: (a) Pt-Sn (60:40) and (b) Pt-Sn (90:10).

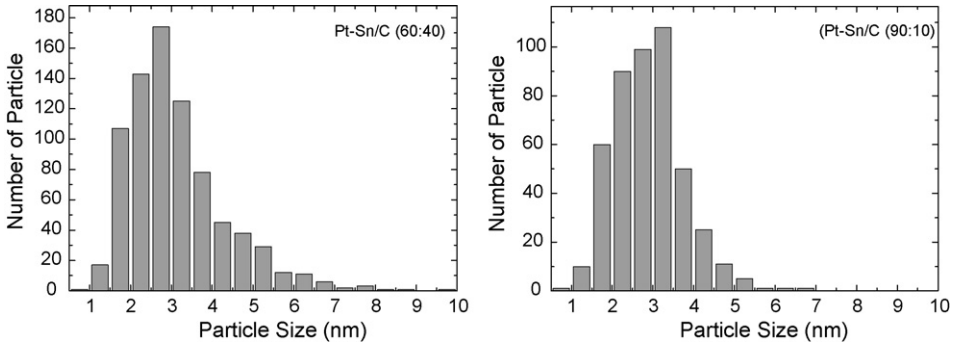

Fig. 3. Histograms of particle size distributions of Pt-Sn/C electrocatalysts (30% metal loading) prepared by thermal decomposition of polymeric precursors.

Table 1
TEM and EDX results of the various bulk compositions of Pt-Sn/C electrocatalysts prepared by thermal decomposition

Catalyst	Nominal content (%)		Determined by EDX (%)		Mean particle size (nm)
	Pt	Sn	Pt	Sn	
Pt-Sn (30% metal loading)	50	50	51.9	48.1	3.2
	60	40	66.5	33.5	3.1
	70	30	72.5	27.5	3.4
	80	20	79.6	20.4	3.3
	90	10	84.5	15.5	2.9

the particles seem smaller in the case of the $Pt_{0.9}Sn_{0.1}$/C catalyst than in the case of the $Pt_{0.6}Sn_{0.4}$/C catalyst (Fig. 2). However, the size distribution presented in Fig. 3 indicates that the mean particle sizes are close for both catalysts (3.0 nm), whereas the dispersion is higher for the Sn-rich catalyst, the mean apparent particles sizes D_m, D_s and D_v being, respectively, 3.1, 4.2 and 4.8 for $Pt_{0.6}Sn_{0.4}$/C (Fig. 3a) and 2.9, 3.1 and 3.7 nm for $Pt_{0.9}Sn_{0.1}$/C (Fig. 3b).

EDX analysis demonstrated the presence of both Pt and Sn in each sample, thereby indicating that bimetallic catalysts were obtained. Analysis of Table 1 shows that the average atomic composition of the different catalysts is close to the theoretical one. It is well known that one of the major causes of performance decay under working conditions is the activity loss due to the particle agglomeration [21,22], among other problems as loss of platinum, Pt/Sn rearrangement or poisoning. TEM images performed on several areas of the samples showed that some zones of the catalysts display large particles, probably due to agglomeration during the calcination step at 400 °C. The mean particle size is around 3 nm (Table 1).

3.2. Electrochemical characterization of the catalysts

Fig. 4 shows cyclic voltammograms for ethanol oxidation on Pt and Pt-Sn/Ti catalysts. All the current values were normalized by the geometric surface area of the electrodes. The true surface area was calculated using the charge of hydrogen adsorption/desorption, allowing the comparison of the different electrodes. Calculation of the true surface areas was confirmed by CO stripping experiments (the adsorption potential was set at 50 mV RHE^{-1}), taking into account that this charge corresponds only to the adsorption of linear CO (CO_L), as it will be shown below. It can be deduced that the painting process and the calcination step lead to a great roughness factor for the catalysts, as presented in Table 2. This factor is the ratio between the true surface area of the catalyst and the geometric surface area of the Ti plate (2 cm^2), if we consider that hydrogen or CO_L adsorption occurs only on the Pt sites.

It can be clearly observed in Fig. 4 that there are two oxidation peaks for ethanol oxidation in the investigated potential range. These peaks shift according to the tin content in the electrocatalysts. In the examples given in Fig. 4, the increase in tin content represents potential gain, i.e., a shift toward lower potentials, whatever the potential scan. Ethanol oxidation on Pt-alone starts at ca. 0.5 V RHE^{-1} while on Pt-Sn catalysts oxidation occurs earlier, i.e., at ca. 0.35 V, which indicates that the modifications induced on Pt by the presence of Sn improves the performance of the Pt-Sn electrode materials. The first peak appears at a potential where surface-bound OH is formed on Pt. During the negative potential scan, the currents remain anodic up to 0.27 V. The shape of the second oxidation peak depends slightly on the Sn content. For 40% Sn content, this peak is located at 0.7 V on the remaining Pt-OH sites, i.e., after desorp-

Table 2
Roughness factor of different electrocatalysts deposited onto a Ti plate of geometric surface area 2 cm^2

Electrode	Roughness factor
Pt	139.6
Pt-Sn (50:50)	127.1
Pt-Sn (60:40)	189.5
Pt-Sn (70:30)	213.2
Pt-Sn (80:20)	195.5
Pt-Sn (90:10)	121.3

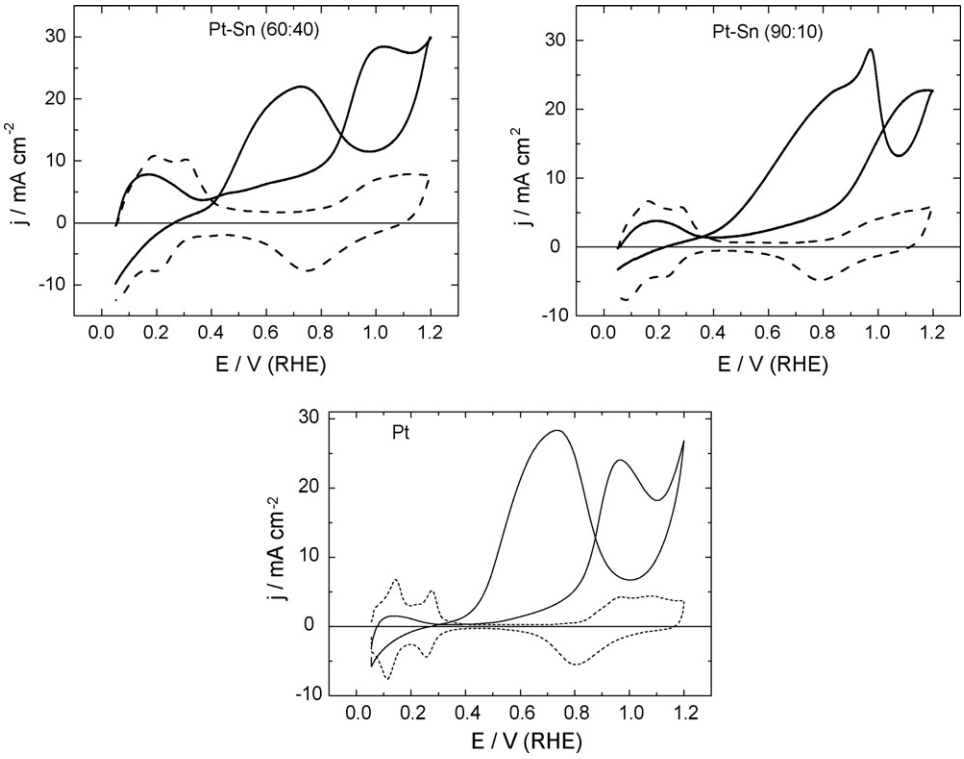

Fig. 4. Cyclic voltammograms of the PtSn/Ti electrodes at 50 mV s^{-1} in a (- - -) 0.5 M H_2SO_4 solution, and in a (—) 0.5 M H_2SO_4 + 0.2 M ethanol solution.

tion of the oxide species from the electrode surface, whereas in the case of 10% Sn content, it is situated at 0.95 V followed by a large shoulder.

Another example of the electroactivity of Pt-Sn nanoparticles for ethanol oxidation is presented in Fig. 5. The effect of tin content in the catalyst composition can be seen during the positive-going scan. As pointed out by several reports in the literature, the presence of a transition metal such as Sn can promote ethanol oxidation by either an electronic effect in the Pt-based electrode material [22–24] or by activation of the interfacial water molecules necessary to promote completion of the oxidation of adsorbed CO leading to CO_2, and of acetaldehyde to acetic acid [24]. It appears that under steady-state conditions, Pt-Sn (60:40) is the electrode material which presents the best activity for ethanol oxidation (see Fig. 5). Considering higher Sn contents it is known that an Sn atomic content larger than 50% inhibits alcohol electrooxidation [16]. So, 40% Sn seems to be the best condition for the removal from the electrode surface of the adsorbed residues formed during the dissociative adsorption of ethanol by adsorbed OH species present on oxidized Sn sites.

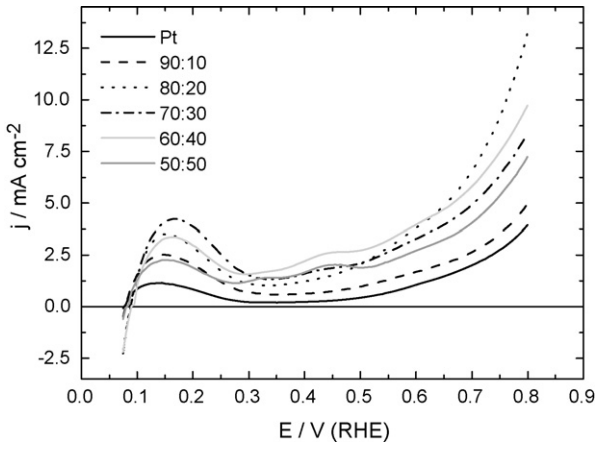

Fig. 5. Electrooxidation of ethanol on Pt-Sn/Ti catalysts. Effect of the composition in tin of the PtSn catalyst; 0.5 M H_2SO_4 + 0.2 M ethanol; at 50 mV s^{-1} and at 21 °C.

3.3. Ethanol electrooxidation under steady-state conditions

Chronoamperometric experiments were carried out at 0.5 V RHE^{-1} for 5 h, to compare the activity of electrocatalysts with different tin contents (Fig. 6). The pattern of current decay is different for different electrocatalysts. $Pt_{60}Sn_{40}$/Ti displays the best electroactivity, as found above in the CV experiments, and its performance is in agreement with that reported by Liu et al. [16]. For long-term operation, PtSn/Ti electrodes show quite stable currents for ethanol oxidation after 150 min while the Pt-alone catalyst continue its decay toward zero current. The origin of the continuous decay can be associated to the accumulation of reaction intermediates in higher amount on the Pt surface than that of Pt-based catalysts, which is supported by the concepts discussed so far.

At the end of the chronoamperometric measurements in a batch cell, the electrolytic solution was analyzed by HPLC. As presented in Table 3, acetaldehyde and acetic acid were mainly formed on the Pt-Sn/Ti surface. The presence of CO_2 trapped in the NaOH solution can also be observed. Traces of formic acid were also determined in the bulk solution, which demonstrates

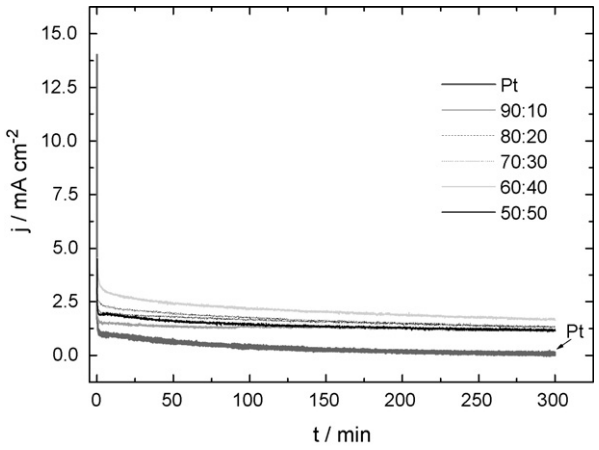

Fig. 6. Current vs. time plots for the electrooxidation of 0.2 M ethanol in 0.5 M H_2SO_4 at 0.5 V RHE^{-1} on various Pt-Sn/Ti electrocatalysts.

the cleavage of the C–C bond of the initial molecule. The mass balance was calculated by measuring the molar quantity of each reaction product as follows:

$$(\%) = \frac{1}{\nu} \times \frac{C_i}{C_0 - C_t} \times 100,$$

where C_0 is the initial concentration of the substrate, C_t its remaining concentration at the end of the chronoamperometric experiment, C_i the concentration of the considered compound and ν is the stoichiometric number.

Mass balances lower than 100% are mainly due to the difficulty in the detection of acetaldehyde. Indeed, as mentioned above in the experimental details, determination of the reaction products was performed by taking into account the cross over process through the ion-exchange membrane to the cathodic side and by comparing the response of each sample with that of a standard reference. Acetaldehyde is very volatile and whatever the precautions taken for optimizing the handling of this molecule (flask and compound at ca. 4 °C), there is no guarantee of total quantification. Acetaldehyde formed and not yet transformed into acetic acid could have been lost in the CO_2 trap circuit. Moreover, esterification can occur with the presence of acetic acid and ethanol in acid medium. Despite these problems, the chromatographic analysis detected the presence of the oxidation products in the bulk solution.

3.4. Performance of the catalysts in the fuel cell

The performance of single fuel cells with different Pt-Sn/C samples as anode catalysts was studied. Typical behaviors are given in Fig. 7 for $Pt_{90}Sn_{10}$. The open-circuit voltage (OCV) of the single fuel cells with different Pt-Sn/C catalysts is given in Table 4.

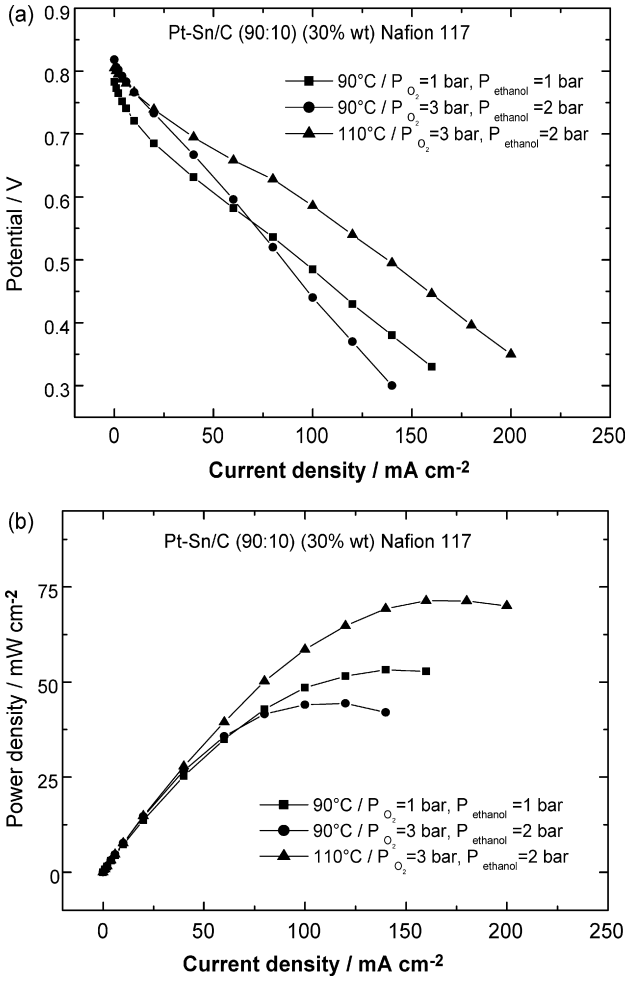

Fig. 7. Performances of single 5 cm^2 DEFC using Pt-Sn/C (90:10, 30% metal loading) under different conditions. (a) Cell voltage against current density; (b) power density against current density.

The average power density obtained for the Pt-Sn/C catalysts investigated is around 50 mW cm^{-2} (Table 4), with $Pt_{90}Sn_{10}$/C exhibiting the highest power density in the single fuel cell (71.8 mW cm^{-2}).

From the electrochemical characterization (cyclic voltammetry and chronoamperometry) it was found that Pt-Sn (60:40) is the best catalyst for ethanol oxidation. On the other hand, under the fuel cell operation conditions the Pt-Sn (90:10) catalyst exhibits the highest activity. Apparently, these observations

Table 3
Distribution of the reaction products determined by HPLC during the oxidation of 0.2 M ethanol at 0.5 V RHE^{-1} on Pt-Sn/Ti electrodes

Electrode Pt-Sn	Ethanol consumed (mM)	Acetic acid (%)	Acetaldehyde (%)	CO_2 (%)	Mass balance (%)
90:10	9.8	7.5	88.5	1.0	97.0
80:20	15.4	8.2	82.6	2.3	93.1
70:30	15.2	10.0	86.3	1.0	97.2
60:40	20.4	18.3	77.5	1.0	97.0
50:50	11.0	10.5	78.8	2.7	92.0

Table 4
Summary of the performances of DEFC with different Pt-Sn/C catalysts at 110 °C

Catalyst	OCV (V)	Current density (mA cm^{-2})	Power density (mW cm^{-2})
$Pt_{90}Sn_{10}$/C	0.81	160.1	71.8
$Pt_{80}Sn_{20}$/C	0.79	120.0	51.8
$Pt_{70}Sn_{30}$/C	0.81	180.1	55.7
$Pt_{60}Sn_{40}$/C	0.77	159.9	49.0
$Pt_{50}Sn_{50}$/C	0.76	140.6	42.3
Pt/C*	0.50	60.0	7.5

looks like contradictory. But, it has to be considered that fuel cell tests were carried out at high temperature, while the electrochemical characterizations were performed at room temperature. Therefore, the comparison of the catalytic activities in these two different systems does not seem appropriate. Additionally, it was previously reported that steady-state conditions, as expected in chronoamperometric experiments, are never achieved on immersed single electrodes and the current values are much lower than the steady-state currents reached under fuel cell testing [25,26]. The reason for this discrepancy is due to several different factors that are difficult to rationalise simultaneously.

3.5. Spectroelectrochemical study of the catalysts

Using the single potential alteration infrared reflectance spectroscopy (SPAIRS) technique, reflectivities were recorded at 50 mV intervals during the first voltammetric scan, at a low sweep rate (1 mV s^{-1}). With the SNIFTIRS technique, spectra were recorded in the whole potential range at constant potential modulation ($\Delta E = 300$ mV). Fig. 8 shows some interesting SPAIRS (Fig. 8a) and SNIFTIRS (Fig. 8b) spectra obtained for ethanol oxidation on Pt-Sn/Au (60:40) nominal composition.

Different absorption bands corresponding to the main reaction products and the intermediates adsorbed are shown in Fig. 8a. A first one appears around 1650–1750 cm^{-1}. This complex band was attributed to the vibration of two different species, the interfacial water (1640 cm^{-1}) and to acetaldehyde and/or acetic acid (stretching mode ν_{CO} from the carbonyl group around 1720 cm^{-1}). An absorption band was also observed at 1470 cm^{-1}. It was assigned to the symmetric OCO stretching mode (ν_sOCO) of the adsorbed acetate ions [32]. There is another band at 1361 cm^{-1} which can be attributed to the CH_3 in plane bending of the adsorbed acetate (δCH_3). For all the samples analyzed here we observed that a bipolar band, due to linearly bonded CO (CO_L) (2035 cm^{-1}), appears from the lowest potential. The domain of linear CO was enlarged with the SNFTIRS technique to observe well its presence during ethanol oxidation on PtSn bimetallic catalysts (Fig. 8b). The presence of the CO_L-band also indicates that ethanol adsorption is dissociative. Moreover, the progressive decrease in the magnitude of the CO-band shows that adsorbed CO_L undergoes further oxidation to CO_2. Conversely, a band which corresponds to the final reaction product CO_2 can be observed at 2345 cm^{-1}. Although it was less intensive than that of CO, it also started appearing at the lowest potential of 200 mV. This behaviour can be explained

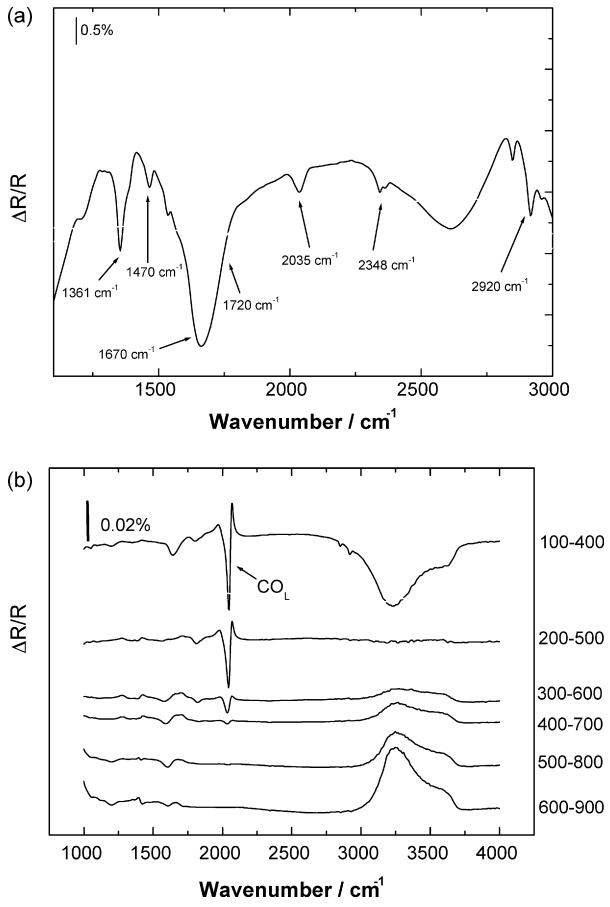

Fig. 8. (a) SPAIR spectra of the species resulting from adsorption and oxidation of 0.1 M ethanol in 0.5 M H_2SO_4 on a Pt:Sn 60:40 electrode at different potentials. (b) SNIFTIR spectra of the species resulting from adsorption and oxidation of 0.1 M ethanol in 0.5 M H_2SO_4 on a Pt:Sn 60:40 electrode at different modulations.

by the bifunctional mechanism that occurs on the Pt-Sn surface at potentials lower than those for Pt-alone. Some other weak bands could be seen at about 2920 cm^{-1} for ν_{CH} of methyl group (CH_3).

Fig. 9 shows the integrated band intensities from SNIFTIRS and SPAIRS spectra for CO_L and CO_2, respectively, as a function of potential. The intensity of the adsorbed CO_L-band is relatively high at 0.2 V and increases significantly up to 0.4 V. For higher potentials CO_L is rapidly consumed up to 0.8 V. Coincidentally, the formation of CO_2 starts at lower potentials than 0.4 V. The formation of CO_2 reaches a maximum at 0.7 V and diminishes slightly up to 0.8 V. From this behavior it can be inferred that CO_2 production started early, confirming CO removal by oxidation on Pt-Sn, which activates interfacial water at low potentials. The decrease in the CO_L-band was proportional to the increase in the CO_2, band suggesting that its formation is mainly due to oxidation of adsorbed CO.

As pointed out above, CH_3CHO, CH_3COOH and CO_2 were the different products detected by in situ reflectance spectroscopy and chromatographic techniques during ethanol oxidation on PtSn catalysts. Adsorbed CO was also detected spectroscopically and similar species have already been described in previous papers [27–34]. In agreement with these

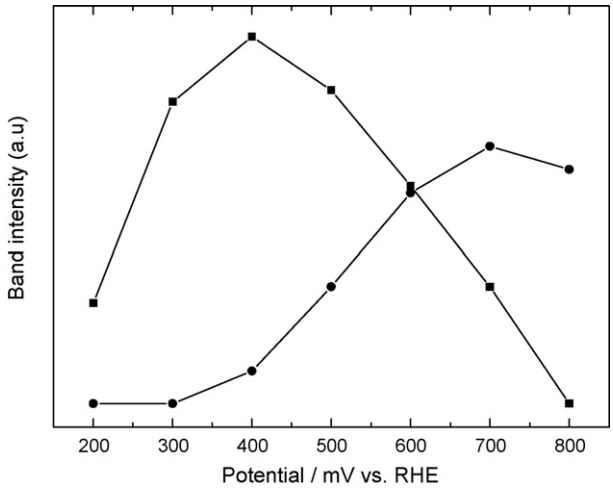

Fig. 9. Integrated band intensity from IR spectra at PtSn/Au catalyst in a 0.5 M H_2SO_4 + 0.1 M CH_3CH_2OH solution. (■) CO_L and (●) CO_2.

results a general scheme for ethanol electrooxidation can be proposed as shown in Scheme 1. First of all, it can be assumed that ethanol adsorbs at the Pt surface followed by the α-C–H dissociation, leading to the formation of adsorbed acetaldehyde, according to steps 1 and 2, that can go to the solution. These way is apparently the simplest reaction step which justify the higher amount of acetaldehyde found in the electrolysis experiments. Acetaldehyde can be readsorbed according to step 3 and the formed adsorbed intermediate can interact with adsorbed OH and generates acetic acid as indicated in step 4. These observations are in accord to the result of electrolysis in which acetic acid is also found in high concentrations. In step 4 the oxidation occurs by a bifunctional mechanism and is not useful for the overall process since it leads to the formation of acetic acid avoiding the total ethanol oxidation towards CO_2. Acetic acid may be formed also following steps 5 and 6 but it is apparently less probable. Fig. 9 shows that CO_L is produced at low potentials and one can consider that its formation takes place through dissociation of the C–C bond of the adsorbed species [24]. The presence of adsorbed CO can be explained by two distinct sequences, i.e., steps 7 and 8 or steps 9 and 10. The first hypothesis implies that ethanol must be adsorbed by the C–H bond rupture in both carbons atoms. The subsequent step is the C–C bond break. The second hypothesis implies in the rupture of the C–H bond of the intermediate formed after the acetaldehyde adsorption. The CO_{ads} species can react with adsorbed OH to form CO_2.

It is generally accepted that the CO oxidation on Pt bimetallic catalysts occurs by a bifunctional reaction mechanism [35] and is described as a Langmuir–Hinshelwood type reaction. It can be considered in our case, that interfacial water is activated by Sn surface atoms at lower potentials. To confirm this hypothesis, we recorded voltammograms of a SnO_2/Ti electrode under CO stripping conditions (Fig. 10). The adsorption potential was established at 50 mV RHE^{-1}.

Fig. 9 shows that CO_L is produced at low potentials and one can consider that its formation takes place through the dissociation of the C–C bond of the adsorbed species (steps 7 or 9) [24].

As expected, there was no oxidation peak, but only tin oxide surface transition was observed which can result in the formation of OH adsorbed species, which are necessary to remove Pt-CO_{ads} to CO_2 and to transform adsorbed species such as ethanol and acetaldehyde into acetic acid, at lower potentials.

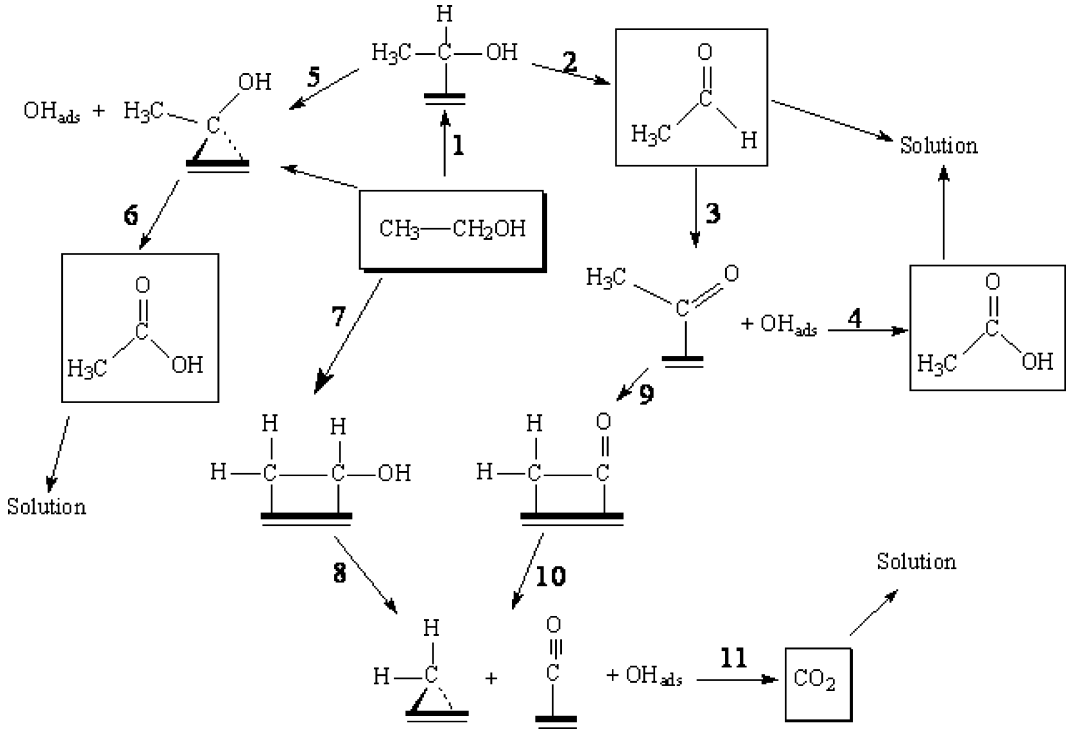

Scheme 1. General scheme of ethanol oxidation on Pt-Sn electrocatalysts.

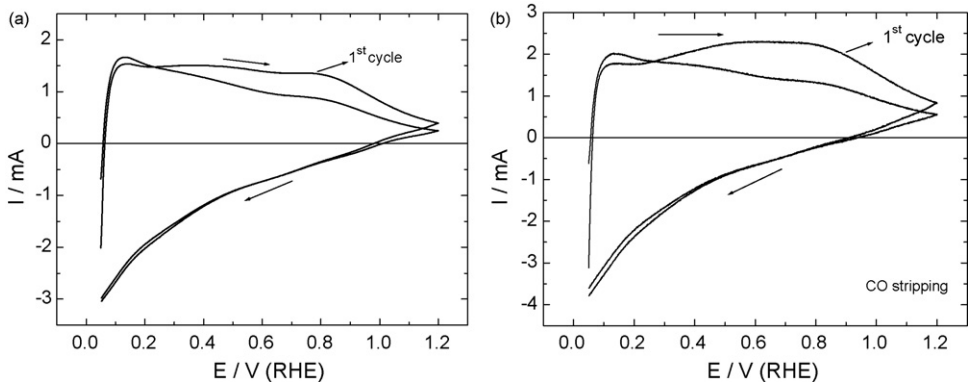

Fig. 10. Voltammograms of a Sn/Ti electrode at 50 mV s^{-1} in a 0.5 M H_2SO_4 solution and in CO stripping conditions: (a) without CO; (b) in the presence of CO.

As pointed out above, chromatographic measurements indicated the presence of CO_2 (and traces of formic acid), which is a sign of the cleavage of the C–C bond during ethanol adsorption on the electrode surface. This CO_2 production as the final reaction product is confirmed by FTIR and HPLC. Fig. 9 shows that the formation of CO_2 is linked to the oxidation of adsorbed CO, which goes through a maximum at around 0.4 V. At this low potential region, it is possible to rationalize that the reaction mechanism of CO removal from the electrode surface occurs with the participation of Sn hydroxides. It can thus be concluded that without Pt in the electrode composition, CO adsorption cannot occur on Sn and all the Pt-Sn catalysts considered in this work are actually $PtSnO_2$ ones in this potential range. These results are in agreement with those obtained on Pt_3Sn electrodes in the literature [36,37]. Experimental observations were supported by density functional theory (DFT) calculations which indicated that on this bimetallic catalyst, CO binds only to Pt atoms and not to the Sn atoms, whereas OH has an energetic preference for the Sn sites.

On the basis of the results presented here, therefore, the preparation of Pt-SnO_n catalysts by thermal decomposition of polymeric precursors and deposited onto various conducting substrates led to enhanced performances for ethanol oxidation. Otherwise, the analysis of the above scheme reveals that the presence of adsorbed OH is necessary in order to oxidize the CO_{ads} species to CO_2 but also that it is present in the step that results in the formation of acetic acid. In that way it is no possible to separate the two contributions of OH_{ads}, i.e., if acetaldehyde is produced, its oxidation in the presence of OH_{ads} will lead to the formation of acetic acid as a parallel product. A ideal catalyst for ethanol oxidation would be one that can result in the selective formation of $CH_2CH(OH)_{ads}$ species by the cleavage of C–H bonds (step 7) followed by the C–C bond cleavage (step 8) and subsequent oxidation of intermediates to CO_2 in the presence of adsorbed OH.

4. Conclusions

The Pt-SnO_2 catalysts studied here display electrocatalytic activity with respect to ethanol oxidation as evidenced by voltammetric and chronoamperometric measurements. Although ethanol oxidation involves theoretically 12 electrons per ethanol molecule when totally oxidized to CO_2, the obtained results showed that its electrocatalytic oxidation on Pt-SnO_2 catalysts led mainly to acetaldehyde and acetic acid. Adsorbed intermediates such as CO_L and CO_2 were also observed by in situ infrared spectroscopy and HPLC analysis (for CO_2). The presence of the last species suggests a rupture of the C–C bond, which occurred during ethanol oxidation on the $PtSnO_2$ catalysts. $Pt_{0.9}Sn_{0.1}O_2$ composition produced the largest power density in a complete fuel cell. A general scheme for ethanol electrooxidation was shown based in the results found here, and it was possible to affirm that the presence of tin was necessary to activate the catalyst and convert CO to CO_2 at lower potentials than those observed on Pt-alone.

Acknowledgements

This work was mainly conducted within the framework of a collaborative programme Comité Français d'Evaluation de la Coopération Universitaire avec le Brésil (CAPES/COFECUB) under grant no. 498/05. The authors acknowledge Mrs L.M.C. Abeid for her help in the preparation of the electrocatalysts. GTF and ERG also acknowledge FAPESP and CNPq, Brazil.

References

[1] Y. Morimoto, E.B. Yeager, J. Electroanal. Chem. 444 (1998) 95.
[2] N. Fujiwara, K.A. Friedrich, U. Stimming, J. Electroanal. Chem. 472 (1999) 120.
[3] C. Lamy, E.M. Belgsir, J.-M. Léger, J. Appl. Electrochem. 31 (2001) 799.
[4] F. Vigier, C. Coutanceau, F. Hahn, E.M. Belgsir, C. Lamy, J. Electroanal. Chem. 563 (2004) 81.
[5] M.B. Oliveira, L.P.R. Profeti, P. Olivi, Electrochem. Commun. 7 (2005) 703.
[6] J.-M. Léger, S. Rousseau, C. Coutanceau, F. Hahn, C. Lamy, Electrochim. Acta 50 (2005) 5118.
[7] J. Guo, T. Zhao, J. Prabhuram, R. Chen, C. Wong, Electrochim. Acta 51 (2005) 754.
[8] G.A. Camara, T. Iwasita, J. Electroanal. Chem. 578 (2005) 315.
[9] L. Jiang, G. Sun, S. Wang, G. Wang, Q. Xin, Z. Zhou, B. Zhou, Electrochem. Commun. 7 (2005) 663.
[10] S. Song, W. Zhou, Z. Zhou, L. Jiang, G. Sun, Q. Xin, V. Leontidis, S. Kontou, P. Tsiakaras, Int. J. Hydrogen Energy 30 (2005) 995.
[11] L. Jiang, Z. Zhou, W. Li, W. Zhou, S. Song, H. Li, G. Sun, Q. Xin, Energy Fuel 18 (2004) 866.

[12] H. Bönnemann, G. Braun, W. Brijoux, R. Brinkmann, A.S. Tilling, K. Seevogel, K. Siepen, J. Organomet. Chem. 520 (1996) 143.
[13] K. Okitsu, A. Yue, S. Tanabe, H. Matsumoto, Chem. Mater. 12 (2002) 3006.
[14] Z.L. Liu, J.Y. Lee, M. Han, W.X. Chen, L.M. Gan, J. Mater. Chem. 12 (2002) 2453.
[15] I. Capek, Adv. Colloid Interface Sci. 110 (2004) 49.
[16] Z. Liu, B. Guo, L. Hong, T.H. Lim, Electrochem. Commun. 8 (2006) 2453.
[17] P. Olivi, E.C. Pereira, E. Longo, J.A. Varela, L.O.S. Bulhões, J. Electrochem. Soc. 140 (1993) L81.
[18] J.C. Forti, P. Olivi, A.R. Andrade, Electrochim. Acta 47 (2001) 913.
[19] A.L. Santos, D. Profeti, P. Olivi, Electrochim. Acta 50 (2005) 2615.
[20] M.M. Besso, US Patent 3,213,120, vol. 3 (1965).
[21] E. Antonili, J. Mater. Sci. 38 (2003) 2995.
[22] T. Iwasita, H. Hoster, A. John-Anacker, W.F. Lin, W. Vielstich, Langmuir 16 (2000) 522.
[23] E.A. Batista, G.R.P. Malpass, A.J. Motheo, T. Iwasita, J. Electroanal. Chem. 571 (2004) 273.
[24] J.M. Léger, Electrochim. Acta 50 (2005) 3123.
[25] M. Goetz, H. Wendt, J. Appl. Electrochem. 31 (2001) 811.
[26] S. Rousseau, C. Coutanceau, C. Lamy, J.-M. Léger, J. Power Sources 158 (2006) 18.
[27] T. Iwasita, E. Pastor, Electrochim. Acta 39 (1994) 531.
[28] S.C. Chang, L.W. Leung, M.J. Weaver, J. Phys. Chem. 94 (1990) 6013.
[29] T. Iwasita, B. Rasch, E. Cattaneo, W. Vielstich, Electrochim. Acta 34 (1989) 1073.
[30] J.M. Perez, B. Beden, F. Hahn, A. Aldaz, C. Lamy, J. Electroanal. Chem. 262 (1989) 251.
[31] A. Rodes, E. Pastor, T. Iwasita, J. Electroanal. Chem. 376 (1994) 10.
[32] M.H. Shao, R.R. Adzic, Electrochim. Acta 50 (2005) 2415.
[33] M. Arenz, V. Stamenkovic, B. Blizanac, K. Mayrhofer, N. Markovic, P. Ross, J. Catal. 232 (2005) 402.
[34] J. Silva-Chong, E. Mendez, J.L. Rodriguez, M.C. Arevalo, E. Pastor, Electrochim. Acta 47 (2002) 1441.
[35] M. Watanabe, S. Motoo, J. Electroanal. Chem. 60 (1975) 259.
[36] T.E. Shubina, M.T.M. Köper, Electrochim. Acta 47 (2002) 3621.
[37] V.R. Stamenkovic, M. Arenz, C.A. Lucas, M.A. Gallagher, P.N. Ross, N.M. Markovic, J. Am. Chem. Soc. 125 (2003) 2736.